

## Direct Observation of Magnetochiral Effects through a Single Metamolecule in Microwave Regions

Satoshi Tomita,<sup>1,\*</sup> Kei Sawada,<sup>2</sup> Andrey Porokhnyuk,<sup>3</sup> and Tetsuya Ueda<sup>3</sup>

<sup>1</sup>Graduate School of Materials Science, Nara Institute of Science and Technology, 8916-5 Takayama, Ikoma, Nara 630-0192, Japan

<sup>2</sup>RIKEN SPring-8 Center, 1-1-1 Kouto, Sayo, Hyogo 679-5148, Japan

<sup>3</sup>Department of Electronics, Kyoto Institute of Technology, Matsugasaki, Sakyo, Kyoto 606-8585, Japan  
(Received 8 June 2014; published 3 December 2014)

We report direct observation of magnetochiral (MCh) effects for the X-band microwaves through a single metamolecule consisting of a copper chiral structure and ferrite rod. A fictitious interaction between chirality and magnetism is realized in the metamolecule without intrinsic electronic interactions. The MCh effects are induced at the resonant optical activities by applying a weak dc magnetic field of 1 mT, and are increased with the magnetic field. The nonreciprocal differences in refractive indices are evaluated to be  $10^{-3}$  at 200 mT.

DOI: 10.1103/PhysRevLett.113.235501

PACS numbers: 81.05.Xj, 78.20.Ek, 78.67.Pt

Symmetry breaking in condensed matter is fascinating in optics [1]. Broken space-inversion and time-reversal symmetries give polarization manipulations, i.e., the optical activities and magneto-optical effects, respectively [2,3]. When both symmetries are simultaneously broken, electromagnetic waves experience the magnetochiral (MCh) effect that is the directional anisotropy independent of polarizations [4–6]. The MCh effect is promising for new functional devices such as a “one-way mirror,” but is very small due to weak coupling between chirality and magnetism in natural materials under a strong magnetic field [7–10]. For optically active organic liquids, variations in refractive indices due to the MCh effects in the visible region were measured to be  $10^{-8}$  at 5 T [11] and  $10^{-10}$  at 100 mT [12] using interferometric detection. Hence it becomes important and interesting to enhance the MCh coupling using artificial structures.

Artificial materials composed of structures much smaller than the wavelength of electromagnetic waves are called metamaterials [13]. One of the important features of metamaterials is a combination of electric and magnetic responses that give interesting phenomena, for example, a negative index of refraction [13] and cloaking [14]. Such phenomena in metamaterials are realized by controlling independently the electric permittivity and magnetic permeability,  $\epsilon$  and  $\mu$ . This independent control of electric and magnetic responses is owing to the absence of an intrinsic interaction between  $\epsilon$  and  $\mu$  in a material. Even without the interaction, electromagnetic waves “feel”  $\epsilon$  and  $\mu$  combined together as a fictitious interaction: a refractive index  $n = \sqrt{\epsilon\mu}$  and wave impedance  $\eta = \sqrt{\mu\mu_0/\epsilon\epsilon_0}$ , where  $\epsilon_0$  and  $\mu_0$  are permittivity and permeability of vacuum, respectively.

In this Letter, we demonstrate the existence of a fictitious interaction between chirality and magnetism as the MCh effect, which includes the cascade MCh effect called in

Ref. [8]. Most studies on directional anisotropy [7,11,12,15–20] have been devoted to realizing and enhancing intrinsic electronic interaction such as magneto-electric resonances. However, we find that the MCh effect occurs in the artificial structure—metamolecule—without using such intrinsic electronic interactions. A large MCh effect by the single metamolecule consisting of a metallic chiral structure and ferrite rod is directly observed in the X-band microwave regions under a very weak magnetic field of 1 mT. The effect can be enhanced by increasing the field and constructing bulklike MCh metamaterials. The nonreciprocal differences in the real and imaginary parts of refractive indices due to the MCh effects are evaluated to be  $10^{-3}$  at 200 mT. The present study paves the way toward the realization of an artificial gauge field for electromagnetic waves using metamaterials [21,22].

Let us consider wave propagation in the microwave region through an isotropic chiral and magneto-optical medium with a chiral parameter  $\xi$  and a magneto-optical parameter  $\kappa$  in the magnetic permeability tensor  $\hat{\mu}$ . Constitutive equations of the electric flux density  $\vec{D}$  and magnetic field  $\vec{B}$  are described using the electric field  $\vec{E}$  and magnetic field strength  $\vec{H}$  as follows [23]:

$$\vec{D} = \epsilon_0 \epsilon \vec{E} - i \frac{\xi}{c} \vec{H}, \quad \vec{B} = \mu_0 \hat{\mu} \vec{H} + i \frac{\xi}{c} \vec{E}. \quad (1)$$

When an external magnetic field is applied in the  $z$  direction,  $\hat{\mu}$  is represented by

$$\hat{\mu} = \begin{pmatrix} \mu & -i\kappa & 0 \\ i\kappa & \mu & 0 \\ 0 & 0 & 1 \end{pmatrix}. \quad (2)$$

Substituting Eqs. (1) and (2) into Maxwell’s equations for a plane wave with  $\vec{k} = (0, 0, k)$  and angular frequency  $\omega$ ,

and using the dispersion relation  $\omega = c|\vec{k}|/n$ , we obtain an index of refraction as

$$n = \sqrt{\epsilon}\sqrt{\mu} \pm \frac{\kappa}{2}\sqrt{\frac{\epsilon}{\mu}} \pm \xi \text{sgn}(k) - \frac{\kappa\xi \text{sgn}(k)}{\mu}, \quad (3)$$

where  $\pm$  represent left- and right-handed circular polarizations. Equation (3) is applicable to electromagnetic waves in the microwave region. In the visible region, one can obtain a similar expression by using off-diagonal components of the electric permittivity instead of those of magnetic permeability.

The right-hand side of Eq. (3) consists of four terms. The first, second, and third terms correspond, respectively, to the conventional refraction, magneto-optical effects, and optical activities. The fourth term representing the cross effect of the optical activities and magneto-optical effects is assigned to the MCh effects. This term is independent of the polarization but dependent on the propagating direction. The MCh effects can be enhanced by a resonance of chirality and/or magnetism. It is important to notice that  $\xi$  and  $\kappa$  have no intrinsic coupling. However, Eq. (3) points out that the electromagnetic waves “regard”  $\xi$  as being coupled to  $\kappa$ .

The MCh metamolecule was embodied by using a copper (Cu) chiral structure and ferrite rod as shown in Fig. 1(a). As illustrated on the right-hand side, the cross section and length of the ferrite rod was  $1.5 \times 1.5$  mm and 15 mm, respectively. A Cu wire of 0.55 mm in diameter was coiled clockwise four times round the thread groove of the right-handed screw to form the chiral structure as shown in the left part. The metamolecule was fixed in a thermal-contraction tube.

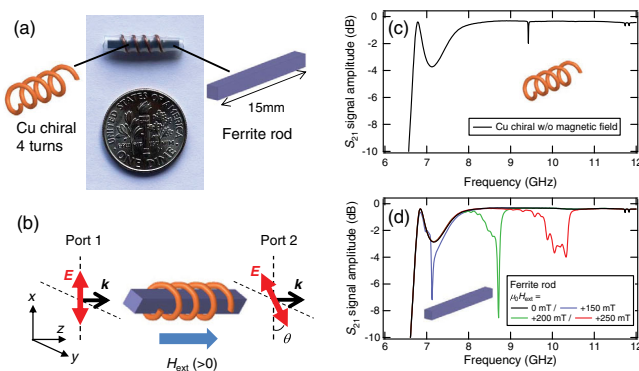


FIG. 1 (color online). (a) Center: A photograph of the MCh metamolecule. Diameter of the coin in the photo is 17.91 mm. Illustrations of Cu chiral structure (left) and ferrite rod (right). (b) A schematic of configurations in the microwave measurements of  $S_{21}$  of the MCh metamolecule. Transmission  $S_{21}$  amplitude spectra of (c) Cu chiral structure without the external magnetic field, and of (d) ferrite rod without the dc field (black), with +150 mT (blue), +200 mT (green), and +250 mT (red).

The sample was put into a WR-90 waveguide terminated at both ends by Agilent 281A coaxial adaptors. Two adaptors were connected via the waveguide so that the polarization plane of the electric field of the fundamental  $TE_{10}$  mode in an adaptor was parallel to that in the other adaptor. The sample in the waveguide was placed between two poles of an electromagnet providing the dc magnetic field,  $H_{\text{ext}}$ , that was monitored by using a Gauss meter equipped with a Hall element. An X-band microwave source was an Agilent PNA N5224 vector network analyzer. We measured the  $S$  parameters of  $S_{21}$ , from port 1 to 2, and  $S_{12}$ , from port 2 to 1, corresponding to transmission coefficients from both sides of the samples in the waveguide. The external dc magnetic field was applied in the  $z$  direction [Fig. 1(b)].

Figure 1(c) shows an amplitude spectrum of  $S_{21}$  in frequencies between 6 and 12 GHz through only the Cu chiral structure without the dc magnetic field. The measurements are valid in the pass band above 6.6 GHz, which is the cutoff frequency of the waveguide. We observe a notch at 9.4 GHz, which is traced back to the resonance of the chiral structure. It gives rise to the optical activity and enhances the activity by resonance [24]. The spectrum of the chiral structure under the applied magnetic field is the same as that shown in Fig. 1(c).

Amplitude spectra of  $S_{21}$  of the ferrite rod are shown in Fig. 1(d). Without the external dc magnetic field, a featureless spectrum (black curve) is obtained between 7 and 12 GHz. Contrastingly, a large notch emerges at 7.1 GHz when the dc field of +150 mT is applied by using the electromagnet (blue curve). This notch shifts to a higher frequency at approximately 8.7 and 10.3 GHz, with an increase in the magnetic field to +200 mT (green curve) and +250 mT (red curve), respectively. The features shifting upward with an increase in the magnetic field originate from the ferromagnetic resonance of the ferrite rod. The main peak of the ferromagnetic resonance accompanies subsidiary peaks at a lower frequency region due to spin-wave resonance in the ferrite rod.

By combining the Cu chiral structure with the ferrite rod and applying the dc magnetic field, we can break both space-inversion and time-reversal symmetries. This simultaneous breaking leads to emergence of the artificial MCh effects as demonstrated in Fig. 2. Figures 2(a)–(c) show amplitude spectra of  $S_{21}$  (red curves) and  $S_{12}$  (blue curves) of the metamolecule under the dc magnetic fields of 0 mT, +10 mT, and +180 mT, respectively. Figures 2(d)–(f) are corresponding phase spectra. For 0 mT, we observe a salient notch at 10.2 GHz and an additional weak notch at 7.5 GHz in Fig. 2(a). The phase spectra in Fig. 2(d) show weak dispersion-type features at these frequencies. These are resonant optical activities due to the Cu chiral structure. The insets in Figs. 2(a) and 2(d) correspond to enlarged spectra at the resonant optical activity at approximately 10 GHz. The inset clearly shows that  $S_{21}$  and  $S_{12}$  spectra are

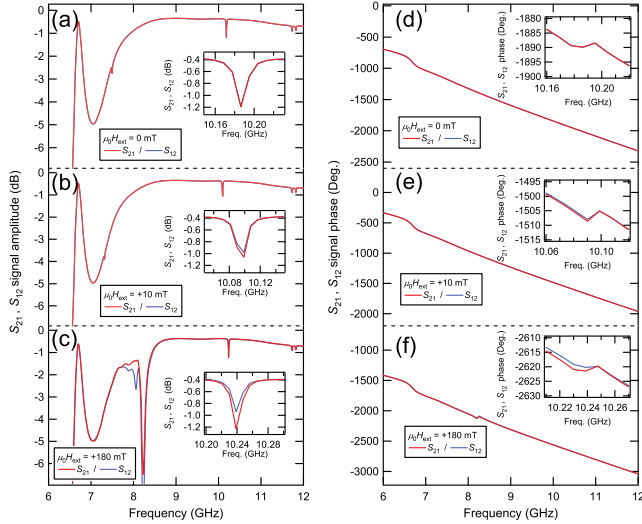


FIG. 2 (color online). Transmission  $S_{21}$  (red) and  $S_{12}$  (blue) amplitude spectra (a)–(c) and phase spectra (d)–(f) of the single MCh metamolecule under the external dc magnetic fields of 0 mT [(a) and (d)], +10 mT [(b) and (e)], and +180 mT [(c) and (f)]. Insets: enlarged spectra at the resonant optical activity around 10 GHz.

identical at 0 mT, namely, in the presence of the time-reversal symmetry.

The artificial MCh effect is manifest in the difference of the transmission amplitude and phase spectra. Indeed, with the applied dc magnetic field of +10 mT, transmission  $S_{21}$  (red) and  $S_{12}$  (blue) spectra at the resonant optical activity are not identical in Figs. 2(b) and 2(e), whether the incident directions of microwaves are parallel or antiparallel to the dc magnetic field. Note that the ferromagnetic resonance is located at a very low frequency of about 1 GHz for +10 mT. Nevertheless, a finite difference between  $S_{21}$  and  $S_{12}$  spectra is observed at the resonant optical activity in Figs. 2(b) and 2(e).

Figures 2(c) and 2(f) show transmission  $S_{21}$  (red) and  $S_{12}$  (blue) spectra with the dc field of +180 mT. We notice that the difference in the spectra around 10 GHz increases. Additionally, complicated features due to ferromagnetic resonance in the ferrite rod emerge at approximately 8 GHz, which shifts to a higher frequency with a further increase in the dc field. A significant difference in amplitude and phase spectra between  $S_{21}$  and  $S_{12}$  is observed at the ferromagnetic resonance. However, this difference is mainly due to an interaction between the asymmetric Cu structure and magnetostatic surface waves of the spin waves. The interaction is similar to the origin of other directional anisotropy, such as optical magnetoelectric effects [25], and is not directly related to the chirality. Therefore in the following, we focus on the MCh effects at the resonant optical activity around 10 GHz.

Further evidence of the MCh effects in the metamolecule is shown in Fig. 3. Plotted are differences in phases

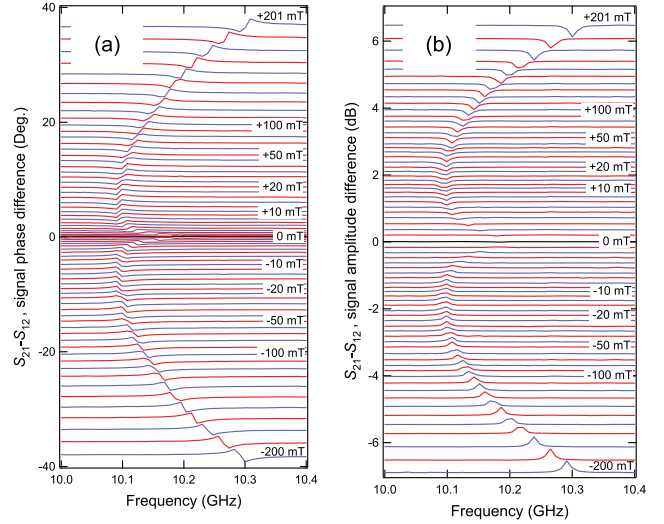


FIG. 3 (color online). Differences in (a) phases and (b) amplitudes between  $S_{21}$  and  $S_{12}$  around 10 GHz of the MCh metamolecule under dc magnetic fields from 0 mT to  $\pm 200$  mT.

[Fig. 3(a)] and amplitudes [Fig. 3(b)] between  $S_{21}$  and  $S_{12}$  under dc magnetic fields from 0 mT to  $\pm 200$  mT. A featureless spectrum is obtained with 0 mT (black line). With +1 mT, a signal with Lorentz-type dispersion due to the artificial MCh effect emerges at a frequency of the resonant optical activity around 10 GHz. Interestingly, a very weak magnetic field of +1 mT is enough to induce the MCh effects. The MCh effect around 10 GHz becomes large and shifts with an increase in the magnetic field. Differential spectra for the reversed direction of the external dc magnetic field ( $H_{\text{ext}} < 0$ ) are also shown in the lower half of Fig. 3. The appearance and frequency shift of the MCh effects are very similar to those in  $H_{\text{ext}} > 0$ , whereas, the polarity of MCh effects is flipped with the direction of the magnetic field. Additionally, we confirmed that the observed signal is odd with respect to the chirality of the metamolecule (see the Supplemental Material [26]).

In Fig. 4(a), we plotted the phase difference evaluated as a half value of the peak-to-peak variation at the resonant optical activity around 10 GHz in Fig. 3(a), as a function of  $\mu_0 H_{\text{ext}}$ . In Fig. 4(b), the amplitude difference is also plotted. Orange (green) marks correspond to the MCh effects under  $H_{\text{ext}} > 0$  ( $H_{\text{ext}} < 0$ ). The MCh effects appear at 1 mT, rapidly grows with the magnetic field up to 10 mT, and monotonically increases with the magnetic field. The continuous increase in the MCh effect is consistent with Eq. (3), which theoretically indicates that the artificial MCh effect increases as the magneto-optical effects increase. It is reasonable to think that the magneto-optical effect is proportional to the effective magnetization [27]. Under the unsaturated regime, the magnetization is a function of the applied dc magnetic field. A rapid increase in the MCh effects at a very low magnetic field below 10 mT is thus caused by the soft magnetic nature of the ferrite rod in the

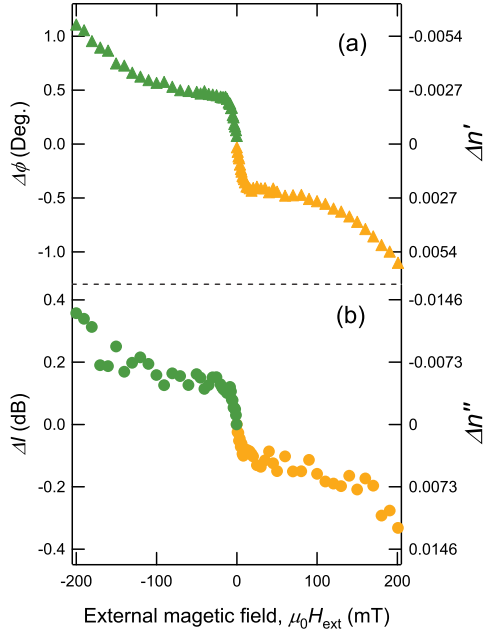


FIG. 4 (color online). Differences in (a) phases and (b) amplitudes are plotted as a function of  $\mu_0 H_{\text{ext}}$ . Evaluated differences in the index of refraction are also indicated from the right axes.

metamolecule that was observed by a magnetometer (see the Supplemental Material [28]).

Finally, we evaluate the difference in refractive indices obtained by the MCh effects. The phase and amplitude differences in the transmission coefficients, as shown in Fig. 4, can be converted to the nonreciprocal differences in the real and imaginary parts of refractive indices  $\Delta n'$  and  $\Delta n''$ , respectively. Consider the 1D structure composed of the single metamolecule inserted in a rectangular waveguide. From Eq. (3), we describe  $\Delta n'$  and  $\Delta n''$  between forward ( $S_{21}$ ) and reverse ( $S_{12}$ ) propagations of unpolarized waves

$$\Delta n = n_{1 \rightarrow 2} - n_{2 \rightarrow 1} = \Delta n' + i\Delta n'' = 2 \frac{\kappa \xi}{\mu}. \quad (4)$$

$\Delta n$  is a Lorentz-type function of the operational frequency and is related to the phase and amplitude of the complex transmission coefficients as follows:

$$\Delta n' = -\frac{c}{2\pi fl} \Delta\phi \approx -47.7 \times \frac{\Delta\phi}{fl}, \quad (5)$$

$$\Delta n'' = -\frac{c}{40\pi(\log_{10} e) fl} \Delta I \approx -5.50 \times \frac{\Delta I}{fl}, \quad (6)$$

where  $\Delta\phi$  denotes the phase difference  $\angle S_{21} - \angle S_{12}$  in radian, and  $\Delta I$  the amplitude difference  $|S_{21}| - |S_{12}|$  in decibel at the MCh effects. The frequency  $f$  is measured

in GHz, and  $l$  represents the total length of the metamolecule measured in millimeters.

At +200 mT, it is found from Fig. 4 that the maximum values of  $\Delta\phi$  and  $\Delta I$  were  $\Delta\phi \sim -1.0^\circ = -0.017$  rad and  $\Delta I \sim -0.4$  dB. From Eqs. (4)–(6), with  $l = 15$  mm and  $f = 10$  GHz, we roughly evaluated  $\Delta n' \approx 5.4 \times 10^{-3}$  and  $\Delta n'' \approx 1.5 \times 10^{-2}$  maxima as indicated from the right axes of Figs. 4(a) and 4(b). The success of the direct observation is attributed to several advantages for the MCh metamolecule in microwave regions: the optical activity is enhanced in the metallic chiral structure [24], the magnetic response of the ferrite rod is large in microwave regions [29], and the microwave phase and amplitude are directly measured using the network analyzer. The manifestation of the real part of the nonreciprocal index difference  $\Delta n'$  and the monotonic increase with the applied magnetic field verifies the MCh effect. The values of  $\Delta n'$  and  $\Delta n''$  of the single metamolecule are not yet considerably large. However, by collecting metamolecules, larger responses are expected. Moreover, our concept of fictitious interaction between chirality and magnetism is applicable to other regions of the spectrum including the visible region.

In conclusion, we demonstrate artificial MCh effects in the X-band microwave region by a single metamolecule consisting of a metallic chiral structure combined with a ferrite rod applied to a dc magnetic field. The MCh effects are induced by a very weak magnetic field of 1 mT and increased with the magnetic field. The nonreciprocal differences in the real and imaginary parts of refractive indices due to the MCh effects are increased up to  $\Delta n' \approx 5.4 \times 10^{-3}$  and  $\Delta n'' \approx 1.5 \times 10^{-2}$  by applying +200 mT.

We thank N. Hosoi, T. Kodama, and M. Hangyo for valuable discussion. The authors acknowledge financial support of this work by MEXT KAKENHI Grants No. 22109002 and No. 22109005, and a grant from the Research Foundation for Opto-Science and Technology.

\*tomita@ms.naist.jp

- [1] E. Hecht, *Optics* (Pearson Education Limited, Essex, 2014).
- [2] J. A. Kong, *Electromagnetic Wave Theory* (EMW Publishing, Cambridge, 2005).
- [3] *Circular Dichroism: Principles and Applications*, 2nd ed., edited by N. Berova, K. Nakanishi, and R. W. Woody (Wiley-VCH, New York, 2000).
- [4] N. B. Baranova, Yu. V. Bogdanov, and B. Ya. Zel'dovich, *Opt. Commun.* **22**, 243 (1977).
- [5] G. Wagnière and M. Meier, *Chem. Phys. Lett.* **93**, 78 (1982).
- [6] L. D. Barron and J. Vrbancich, *Mol. Phys.* **51**, 715 (1984).
- [7] G. L. J. A. Rikken and E. Raupach, *Nature (London)* **390**, 493 (1997).
- [8] G. L. J. A. Rikken and E. Raupach, *Phys. Rev. E* **58**, 5081 (1998).
- [9] V. Krstić, S. Roth, M. Burghard, K. Kern, and G. L. J. A. Rikken, *J. Chem. Phys.* **117**, 11315 (2002).

- [10] V. A. Sautenkov, Y. V. Rostovtsev, H. Chen, P. Hsu, G. S. Agarwal, and M. O. Scully, *Phys. Rev. Lett.* **94**, 233601 (2005).
- [11] P. Kleindienst and G. H. Wagnière, *Chem. Phys. Lett.* **288**, 89 (1998).
- [12] M. Vallet, R. Ghosh, A. Le Floch, T. Ruchon, F. Bretenaker, and J.-Y. Thépôt, *Phys. Rev. Lett.* **87**, 183003 (2001).
- [13] D. R. Smith, J. B. Pendry, and M. C. K. Wiltshire, *Science* **305**, 788 (2004).
- [14] D. Schurig, J. J. Mock, B. J. Justice, S. A. Cummer, J. B. Pendry, A. F. Starr, and D. R. Smith, *Science* **314**, 977 (2006).
- [15] V. A. Markelov, M. A. Novikov, and A. A. Turkin, *Pis'ma Zh. Eksp. Teor. Fiz.* **25**, 404 (1977) [*JETP Lett.* **25**, 378 (1977)].
- [16] C. Train, R. Gheorghe, V. Krstić, L.-M. Chamoreau, N. S. Ovanesyan, G. L. J. A. Rikken, M. Gruselle, and M. Verdaguer, *Nat. Mater.* **7**, 729 (2008).
- [17] I. Kézsmárki, N. Kida, H. Murakawa, S. Bordács, Y. Onose, and Y. Tokura, *Phys. Rev. Lett.* **106**, 057403 (2011).
- [18] S. Bordács, I. Kézsmárki, D. Szaller, L. Demkó, N. Kida, H. Murakawa, Y. Onose, R. Shimano, T. Rőöm, U. Nagel, S. Miyahara, N. Furukawa, and Y. Tokura, *Nat. Phys.* **8**, 734 (2012).
- [19] M. Mochizuki and S. Seki, *Phys. Rev. B* **87**, 134403 (2013).
- [20] I. Kézsmárki, D. Szaller, S. Bordács, V. Kocsis, Y. Tokunaga, Y. Taguchi, H. Murakawa, Y. Tokura, H. Engelkamp, T. Rőöm, and U. Nagel, *Nat. Commun.* **5**, 3203 (2014).
- [21] K. Sawada and N. Nagaosa, *Phys. Rev. Lett.* **95**, 237402 (2005).
- [22] K. Fang, Z. Yu, and S. Fan, *Nat. Photon.* **6**, 782 (2012).
- [23] *Electromagnetic Fields in Unconventional Materials and Structures*, edited by O. N. Singh and A. Lakhtakia (Wiley-Interscience, New York, 2004).
- [24] K. F. Lindman, *Ann. Phys. (Berlin)* **368**, 621 (1920).
- [25] N. Kida, T. Yamada, M. Konoto, Y. Okimoto, T. Arima, K. Koike, H. Akoh, and Y. Tokura, *Phys. Rev. Lett.* **94**, 077205 (2005).
- [26] We used the right-or left-handed metamolecule consisting of a ferrite cylinder and a Cu chiral structure prepared by winding a Cu wire around a metal rod without thread grooves. See the Supplemental Material at <http://link.aps.org/supplemental/10.1103/PhysRevLett.113.235501> for details (Fig. S1).
- [27] C. L. Hogan, *Bell Syst. Tech. J.* **31**, 1 (1952).
- [28] See Supplemental Material at <http://link.aps.org/supplemental/10.1103/PhysRevLett.113.235501> for magnetization curve.
- [29] T. Ueda, S. Yamamoto, Y. Kado, and T. Itoh, *IEEE Trans. Microwave Theory Tech.* **60**, 3043 (2012).